Partial Element Equivalent Circuit Based Parallel Electromagnetic Transient Simulation on GPU

Madhawa Ranasinghe, *Graduate Student Member, IEEE*, and Venkata Dinavahi, *Fellow, IEEE*
Department of Electrical and Computer Engineering, University of Alberta, Edmonton, AB T6G 1H9 Canada

The partial element equivalent circuit (PEEC) method effectively solves Maxwell's equations in integral form by converting electromagnetic field components into the electrical circuit domain. This article proposes a novel transmission line modeling (TLM) based parallel PEEC time-domain solver to solve nonlinear electromagnetic problems. The method substitutes both linear and nonlinear components in the standard PEEC equivalent circuit with corresponding TLM models, leading to an electrical current-based linear network and a magnetic current-based nonlinear network. The proposed TLM-PEEC method effectively decouples the nonlinear elements from the linear network, enabling individual solutions for the nonlinearities and making it highly suitable for parallel processing. Each nonlinear element is solved using parallel Newton-Raphson (N-R) iterations, and the analytical calculation of the Jacobian is presented along with the algorithm. The parallelization of the TLM-PEEC method is explored and implemented on a many-core graphics processing unit (GPU) and a multi-core central processing unit (CPU) to provide detailed field-oriented information on electromagnetic transients in a single-phase 2D shell-type transformer. The proposed architecture was easily coupled with an external network, and the accuracy and computational efficiency of the TLM-PEEC method was verified through similar simulation results obtained from Comsol Multiphysics.

***Index Terms*—Circuit modeling, computational electromagnetics, electromagnetic transients, graphics processing units (GPUs), integral equations, nonlinear systems, parallel processing, partial element equivalent circuit (PEEC) method, time-domain solver, transformer modeling, transmission line modeling (TLM) method.**

I. Introduction

THE electromagnetic numerical modeling of power systems apparatus has been widely adopted in various industries due to its effectiveness and accuracy. Over the years several methods have been employed to model power system apparatus. The finite-element method (FEM) has been extensively utilized in combination with hybrid methods such as finite element/boundary integral method [1], [2] and finite-element/transmission line modeling (TLM) method [3], [4] for modeling power systems. The broad usage of FEM in power system modeling is mainly due to its capability to handle complex geometries while ensuring higher precision.

More recently, integral equation methods have emerged as a viable approach for electromagnetic simulation in power systems [5], [6]. Integral-based numerical methods are advantageous over differential methods as they eliminate the need for meshing the air region, while the conductors, dielectrics, and magnetic materials are required to be meshed. Therefore, integral-based numerical methods require a fewer number of elements and unknowns compared to differential methods, contributing to their computational efficiency.

The partial element equivalent circuit (PEEC) method [7]–[9] performs a crucial role among integral-based numerical methods due to their ability to transform the electromagnetic field problem into an equivalent circuit problem that can be efficiently solved using circuit solvers. The PEEC method was initially introduced for multi-conductor systems and later it has been extended to model dielectric materials [10]. Interconnect analysis of fast-switching electronic devices have widely been performed using this method due to its capability to handle a broader frequency range while expressing parasitic inductances and capacitances using electrical circuits [11].

Authors have recently introduced the PEEC method for linear magnetic materials [12] allowing it to be applied in solving magnetization currents. Comprehensive mathematical models for linear magnetic materials are published in [13] and later it has been further developed to model non-linear magnetic materials [14]. The PEEC magnetic models can be represented using an equivalent circuit model similar to that used for conductors. These models consist of an additional voltage source that corresponds to the effect of magnetization currents within the magnetic material.

In the PEEC framework, systems can be solved either in time-domain or frequency-domain although time-domain solution is of great benefit for transient simulations, particularly for non-linear systems. A PEEC non-linear time-domain solver is presented in [14], and the solution of the non-linear system is based on the vector Newton-Raphson (N-R) algorithm, which is supported by the explicit computation of the Jacobian matrix. Additionally, the time-domain solver is further improved by incorporating an algorithm that dynamically adjusts the time step during transient analysis. This adaptive time-step algorithm enables the solution to be expedited without compromising accuracy.

The modified nodal analysis (MNA) [15] is widely used in solving the PEEC equivalent circuit network, formulating a matrix system that provides solutions for branch currents and nodal voltages [16]. An MNA-based hybrid PEEC time-domain nonlinear solver is presented in [17], addressing nonlinear electromagnetic problems through an iterative N-

This work was supported by the Natural Science and Engineering Research Council of Canada (NSERC). Corresponding author: Madhawa Ranasinghe.
The authors are with the Department of Electrical and Computer Engineering, University of Alberta, Edmonton, AB T6G 1H9, Canada (e-mail: donlucks@ualberta.ca; dinavahi@ualberta.ca).

R approach for the entire system while employing Taylor's expansion to linearize nonlinear components. As the PEEC method offers a comprehensive electric circuit formulation, the MNA can be effectively employed to achieve a stable solution.

The TLM method was originally developed by Johns et al. [18] to simulate wave propagation, and later it was introduced for the analysis of non-linear networks by decoupling non-linear elements from the linear network [19]–[21]. The decoupling is achieved by connecting non-linear elements to the network through lossless transmission lines. As a result, individual solutions for the non-linear elements can be obtained using the N-R method, instead of employing the vector N-R method for the entire system. This concept has been successfully applied to FEM simulations, demonstrating improvements in both accuracy and computational efficiency.

This paper aims to introduce a novel non-linear PEEC time-domain solver utilizing the TLM method. Although the TLM method is a standalone electromagnetic solver, in our work, we utilize TLM as a decomposition technique to decompose linear and nonlinear systems. The proposed approach aims to isolate the non-linear elements in the PEEC equivalent circuit from the linear network using the TLM method and solve them using N-R iterations. Additionally, inductive and capacitive elements within the PEEC equivalent circuit will be substituted with lossless transmission lines to obtain a discrete time-domain model. The proposed hybrid TLM-PEEC approach differs from the general MNA solver as the method separates the nonlinear circuit components from the equivalent circuit network and provides parallel individual nonlinear iterations. The parallelism of the TLM-PEEC solution has been fully explored to achieve offline PEEC simulation of electromagnetic transients in a 2D single-phase shell-type transformer coupled to an external network. The offline simulation is performed on the Nvidia Tesla V100 GPU and Intel Xeon E5-2698 CPU, and the results are compared with those obtained from the commercial FEM software Comsol Multiphysics® in terms of accuracy and computational efficiency.

This paper is organized as follows. Section II presents the fundamental PEEC formulation for conductors, including non-linear magnetic materials. Section III describes the time-domain solver based on the TLM approach specifically designed for non-linear systems. This section elaborates on the process of decoupling non-linear elements and the integration of the N-R method for these elements. In Section IV, the design of the TLM-PEEC transformer model, along with its detailed implementation on both the GPU and CPU, is provided, including the obtained results. Finally, Section V concludes the paper by summarizing the key insights and contributions.

II. PEEC Formulation

The standard PEEC formulation relies on the total electric field of the material, defined by the electric field integral equation (EFIE) at an observation point $\boldsymbol{r}$ due to the source point $\boldsymbol{r}'$, and is expressed as follows:

$$\boldsymbol{E}_s(\boldsymbol{r},t) = \frac{\boldsymbol{J}(\boldsymbol{r},t)}{\sigma} + \frac{\partial \boldsymbol{A}(\boldsymbol{r},t)}{\partial t} + \nabla\Phi(\boldsymbol{r},t), \tag{1}$$

where $\boldsymbol{E}_s(\boldsymbol{r},t)$ represent the incident external electric field at point $\boldsymbol{r}$ at time t, and σ denotes the electrical conductivity of the material. The electric scalar potential $\Phi(\boldsymbol{r},t)$ can be expressed in terms of the surface charge density $\boldsymbol{q}$ and surface area $\boldsymbol{s}'$ of the material as,

$$\Phi(\boldsymbol{r},t) = \frac{1}{4\pi\varepsilon_0}\int_{S'} \frac{\boldsymbol{q}(\boldsymbol{r},t)}{|\boldsymbol{r}-\boldsymbol{r}'|} ds'. \tag{2}$$

In (1), $\boldsymbol{J}(\boldsymbol{r},t)$ and $\boldsymbol{A}(\boldsymbol{r},t)$ represent the electrical current density and magnetic vector potential, respectively. In the presence of conductors and magnetic materials, $\boldsymbol{A}(\boldsymbol{r},t)$ can be expressed as the vector summation of magnetic vector potential due to conductors and magnetic materials [12] in terms of $\boldsymbol{J}(\boldsymbol{r}',t)$ and magnetization currents $\boldsymbol{M}(\boldsymbol{r}',t)$:

$$\boldsymbol{A}(\boldsymbol{r},t) = \boldsymbol{A}_c(\boldsymbol{r},t) + \boldsymbol{A}_m(\boldsymbol{r},t), \tag{3a}$$

$$\boldsymbol{A}_c(\boldsymbol{r},t) = \frac{\mu_0}{4\pi}\int_{V_c'} \frac{\boldsymbol{J}(\boldsymbol{r}',t)}{|\boldsymbol{r}-\boldsymbol{r}'|} dv_c', \tag{3b}$$

$$\boldsymbol{A}_m(\boldsymbol{r},t) = \frac{\mu_0}{4\pi}\int_{V_m'} \boldsymbol{M}(\boldsymbol{r}',t)\times\nabla'\frac{1}{|\boldsymbol{r}-\boldsymbol{r}'|} dv_m', \tag{3c}$$

where V_c' and V_m' denote the volumes associated with electrical and magnetization currents. The standard PEEC method expands electric current, magnetic current, and charge densities into a series of basis functions. Rectangular basis functions are employed to treat current densities, charge densities, and magnetization currents as constants within the elementary volume or surface cells, ensuring simplicity and efficiency in the calculations:

$$\boldsymbol{J}(\boldsymbol{r},t) = \sum_{i=1}^{N_l} J_i(t)\boldsymbol{f}_i(\boldsymbol{r}_i), \tag{4a}$$

$$\boldsymbol{M}(\boldsymbol{r},t) = \sum_{j=1}^{3N_m} M_j(t)\boldsymbol{b}_j(\boldsymbol{r}_j), \tag{4b}$$

$$\boldsymbol{q}(\boldsymbol{r},t) = \sum_{l=1}^{N_n} Q_l(t)\boldsymbol{p}_l(\boldsymbol{r}_l). \tag{4c}$$

N_l and N_m represent the number of elementary volumes utilized for discretizing the conductor and magnetic materials, respectively. N_n denotes the number of surface cells employed for discretizing the conductor cells containing charges. $\boldsymbol{f}$, $\boldsymbol{b}$, and $\boldsymbol{p}$ represent the unit vectors corresponding to current densities, magnetization currents, and charge densities, respectively. Equations (1) - (4) lead to the representation of discretized EFIE. Galerkin's weighting process is used to formulate a system of equations for solving the unknowns J_i, M_j and Q_k using an orthogonal set of weighting functions aligned with the basis functions. This formulation transforms the discretized EFIE into a system of equations that can be represented as an equivalent circuit comprising partial resistance, partial inductance, and coefficient of potential terms. Pulse basis functions are used in this formulation, allowing the electrical quantities to be treated as constant across the elementary volume or surface cells. Galerkin's formulation transforms the discretized EFIE into the circuit domain, and for the conductor volume cell k, it becomes [13]:

$$v_{s,k}(t) = R_k I_k(t) + \sum_{i=1}^{N_l} L_{p,ki} \frac{\partial I_i(t)}{\partial t} + \sum_{j=1}^{3N_m} L_{m,kj} \frac{\partial M_j(t)}{\partial t} + \sum_{l=1}^{N_n} Q_l(t)(p_{k,l}^{+} - p_{k,l}^{-}), \tag{5a}$$

$$R_k = \frac{l_{ck}}{\sigma a_{ck}}, \tag{5b}$$

$$L_{p,ki} = \frac{\mu_0}{4\pi} \frac{1}{a_{ck}} \frac{1}{a_{ci}} \int_{V_{ck}} \int_{V'_{ci}} \frac{\boldsymbol{f}_k(\boldsymbol{r}_k) \cdot \boldsymbol{f}_i(\boldsymbol{r}'_i)}{|\boldsymbol{r}_k - \boldsymbol{r}'_i|} dv'_{ci} dv_{ck}, \tag{5c}$$

$$L_{m,kj} = \frac{\mu_0}{4\pi} \frac{1}{a_{ck}} \int_{V_{ck}} \int_{V'_{mj}} \left[\boldsymbol{b}_j(\boldsymbol{r}'_j) \cdot \frac{(\boldsymbol{r}_k - \boldsymbol{r}'_j)}{|\boldsymbol{r}_k - \boldsymbol{r}'_j|^3} \right] dv'_{mj} dv_{ck}, \tag{5d}$$

$$p_{kl} = \frac{1}{4\pi \varepsilon_0 S_k S'_l} \int_{S_k} \int_{S'_l} \frac{1}{|\boldsymbol{r}_k - \boldsymbol{r}'_l|} ds'_l ds_k. \tag{5e}$$

R_k denotes the partial resistance of the conductor element k, while $L_{p,ki}$ and $L_{m,kj}$ represent the partial inductances between the conductor element k and the conductor element i and the magnetic material element j, respectively. P_{kl} describes the partial coefficient of potential between the conductor elements k and n. In matrix form (5) can be interpreted as follows:

$$-\mathbf{A}\Phi(t) = \mathbf{V}_s(t) + \mathbf{R}\mathbf{I}(t) + \mathbf{L}_p \frac{d\mathbf{I}(t)}{dt} + \mathbf{L}_m \frac{d\mathbf{M}(t)}{dt}. \tag{6}$$

The Kirchhoff's voltage law (KVL) interpretation of the equivalent circuit model is represented in (6), where $\mathbf{A}$ represents the connectivity matrix and $\mathbf{V}_s(t)$ denotes the voltage sources due to incident fields. $\Phi(t)$, $\mathbf{I}(t)$ and $\mathbf{M}(t)$ represent the nodal potential vector, branch current vector, and magnetization vector, respectively. By enforcing Kirchhoff's current law (KCL) at each node of the PEEC equivalent circuit and using the lumped current sources at each node $\mathbf{I}_s(t)$, the following matrix equation can be obtained:

$$\mathbf{P}^{-1} \frac{d\Phi(t)}{dt} - \mathbf{A}^T \mathbf{I}(t) = \mathbf{I}_s(t). \tag{7}$$

The non-linear constitutive relationship of a magnetic material can be expressed as follows:

$$\boldsymbol{B}(\boldsymbol{r},t) = \mu_0 \mu_r(|\boldsymbol{H}(\boldsymbol{r},t)|) \boldsymbol{H}(\boldsymbol{r},t) \tag{8a}$$

$$\boldsymbol{B}(\boldsymbol{r},t) = \mu_0 (\boldsymbol{H}(\boldsymbol{r},t) + \boldsymbol{M}(\boldsymbol{r},t)) \tag{8b}$$

where $\mu_r(|\boldsymbol{H}(\boldsymbol{r},t)|)$ represents the nonlinear magnetic permeability of the magnetic material. The combination of these two equations yields a relationship between the magnetic vector potential and magnetization currents, which can be expressed as:

$$\nabla \times \boldsymbol{A}(\boldsymbol{r},t) = \frac{\mu_0 \mu_r(|\boldsymbol{H}(\boldsymbol{r},t)|)}{\mu_r(|\boldsymbol{H}(\boldsymbol{r},t)|) - 1} \boldsymbol{M}(\boldsymbol{r},t). \tag{9}$$

$\boldsymbol{A}(\boldsymbol{r},t)$ can be substituted using equation (3), and it can be expanded on conductor and magnetic material elements to derive a vectorial equation, expressed as follows [14]:

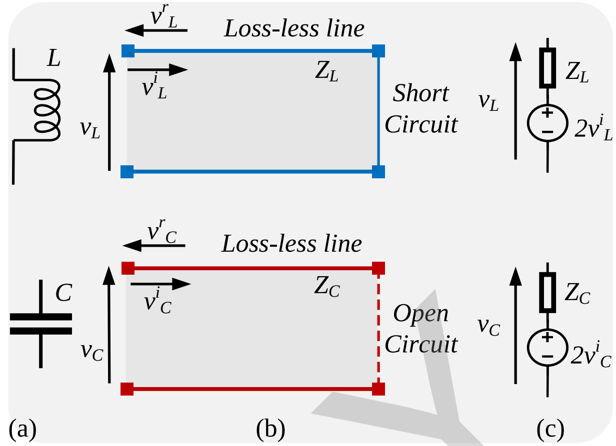

Fig. 1. (a) Linear parasitic element. (b) TLM model. (c) Thevenin equivalent circuit.

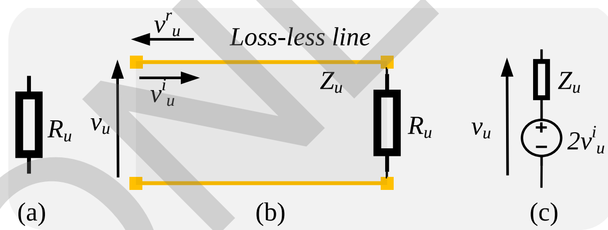

Fig. 2. (a) Non-Linear element. (b) TLM model. (c) Thevenin equivalent circuit.

$$\sum_{i=1}^{N_l} \boldsymbol{D}_{ki} I_i(t) + \sum_{j=1}^{3N_m} \boldsymbol{T}_{kj}(|\boldsymbol{H}_j(t)|) M_j(t) = \sum_{n=1}^{N_{so}} \boldsymbol{G}_{kn} I_{s,n}(t), \tag{10a}$$

$$\boldsymbol{T}_{kj}(|\boldsymbol{H}_j(t)|) = \boldsymbol{W}_{kj} + \Omega_{kj}(|\boldsymbol{H}_j(t)|), \tag{10b}$$

$$\boldsymbol{W}_{kj} = \frac{\mu_0}{4\pi} \int_{V'_{mj}} \nabla \times \left(\nabla \times \frac{\boldsymbol{b}_j(\boldsymbol{r}'_j)}{|\boldsymbol{r}_k - \boldsymbol{r}'_j|} \right) dv'_{mj}, \tag{10c}$$

$$\Omega_{kj}(|\boldsymbol{H}_j(t)|) = -\frac{\mu_0 \mu_r(|\boldsymbol{H}_j(t)|)}{\mu_r(|\boldsymbol{H}_j(t)|) - 1} \hat{u}_{kj}, \tag{10d}$$

$$\boldsymbol{D}_{ki} = \frac{\mu_0}{4\pi} \frac{1}{a'_{ci}} \int_{V'_{ci}} \nabla \times \frac{\boldsymbol{f}_i(\boldsymbol{r}'_i)}{|\boldsymbol{r}_k - \boldsymbol{r}'_i|} dv'_{ci}, \tag{10e}$$

$$\boldsymbol{G}_{kn} = \frac{\mu_0}{4\pi} \frac{1}{a'_{sn}} \int_{V'_{sn}} \nabla \times \frac{\boldsymbol{f}_{sn}(\boldsymbol{r}'_n)}{|\boldsymbol{r}_k - \boldsymbol{r}'_n|} dv'_{sn}. \tag{10f}$$

N_{so} represent the number of elementary sources, $\boldsymbol{f}_s$ accounts for the vector basis functions for the source, and a_{sn} refers to the cross-sectional area of the n_{th} source. $\hat{u}_{kj}$ refers to a unit vector which is 1 for all $k = j$ and 0 for all $k \neq j$. In matrix form, equation (10) can be interpreted as:

$$\mathbf{D}\mathbf{I}(t) + \mathbf{T}(|\mathbf{H}(t)|)\mathbf{M}(t) = -\mathbf{G}\mathbf{I}_s(t). \tag{11}$$

Equations (6), (7) and (11) represent the matrix equation system to solve the PEEC equivalent circuit network.

III. Proposed TLM-PEEC Solution

The PEEC equivalent circuit consists of both linear and non-linear reactive elements. The TLM technique can be employed to model linear reactive elements using their equivalent

This article has been accepted for publication in IEEE Transactions on Magnetics. This is the author's version which has not been fully edited and
content may change prior to final publication. Citation information: DOI 10.1109/TMAG.2024.3447621

discrete-time model while decoupling the non-linear elements from the linear network.

A. TLM Models for Linear Reactive Elements

The surge or characteristic impedance of a loss-less transmission line, represented by $Z_0 = \sqrt{L/C}$, determines whether the line is predominantly inductive or capacitive based on the values of L and C.

A linear inductor can be modeled as a loss-less transmission line that is short-circuited at the far end, with the surge impedance of $Z_L = 2L/\Delta t$ where Δt is the round trip time of the traveling waves on the line. Similarly, a linear capacitor can be modeled as a loss-less transmission line that is open-circuited at the far end, with the surge impedance of $Z_C = \Delta t/2C$. Linear parasitic elements, TLM model, and their respective Thevenin's equivalent circuits are depicted in Fig. 1. ${}_n v_L$, ${}_n v_L^i$, and ${}_n v_L^r$ denote the inductor voltage, incident voltage pulse, and reflective voltage pulse, respectively. Meanwhile, ${}_n v_C$, ${}_n v_C^i$, and ${}_n v_C^r$ represent the similar voltages associated with the capacitor.

According to the transmission line theory, the voltage across the inductor or capacitor can be expressed as the sum of the incident voltage and the reflected voltage. The incident voltage pulse for the next time step can be derived from the reflected voltage pulse and the reflection coefficient at the far end. For a transmission line that is short-circuited at the far end, the reflection coefficient is -1. Hence, in the case of an inductor, the incident voltage pulse for the next time step is $-{}_n v_L^r$. However, when a transmission line is open-circuited at the far end, the reflection coefficient is +1. Consequently, for a capacitor, the incident voltage for the next time step is $+{}_n v_C^r$.

B. TLM Model for Nonlinear Elements

A non-linear element can be separated from the linear network by utilizing a lossless transmission line with an arbitrary surge impedance Z_u, as illustrated in Fig. 2. The voltage across the non-linear resistor at the n^{th} time step can be derived as:

$$ {}_n v_u = Z_u \cdot {}_n i_u + 2 \cdot {}_n v_u^i, \tag{12}$$

where ${}_n v_u^i$ and ${}_n i_u$ represent the incident voltage and line current at the n^{th} time step. According to the transmission line theory, the voltage across the non-linear resistor can be expressed as the sum of the incident and the reflected voltage pulses. Alternatively, if the non-linear relationship of the resistor is expressed as ${}_n v_u = f({}_n i_u)$, the voltage across the non-linear element can be derived as:

$$ {}_{n+1} v_u^i + {}_n v_u^r = f\left(\frac{{}_{n+1} v_u^i - {}_n v_u^r}{Z_u}\right). \tag{13}$$

This is a single non-linear equation that can be solved independently using N-R iterations for the incident pulse of the next time step ${}_{n+1} v_u^i$.

C. TLM Model for the PEEC Circuit

The linear TLM models, along with their corresponding Thevenin equivalent circuit models, can be seamlessly integrated into the PEEC framework, as depicted in Fig. 3.

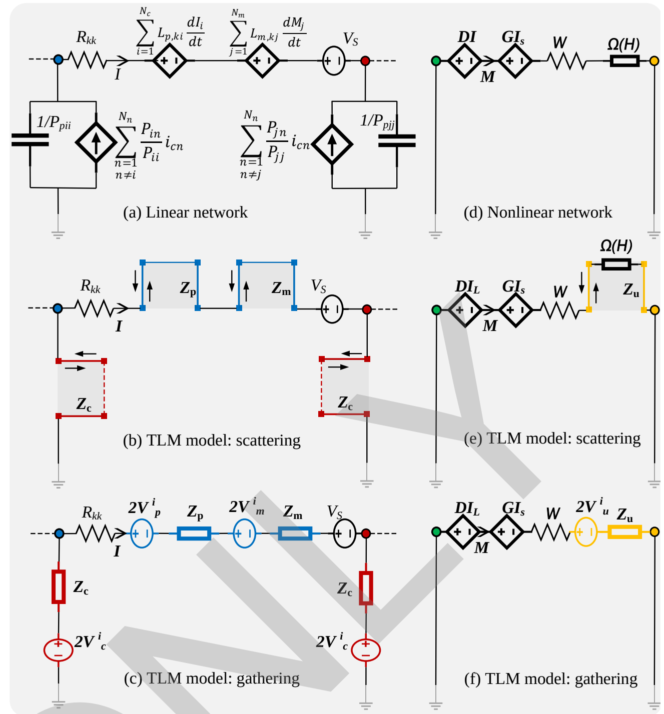

Fig. 3. TLM model of the PEEC equivalent circuit.

The linear inductors and capacitors in the conventional PEEC model have been replaced with lossless transmission lines, which are either short-circuited or open-circuited at their far ends. Fig. 3c depicts the Thevenin equivalent model of this configuration. The solution for this system is achieved in the time domain, utilizing the TLM iterations. According to the TLM model, the equivalent representation of equation (6) can be rewritten as:

$$ \begin{aligned} -\mathbf{A}\Phi(t) = \mathbf{V}_s(t) + \mathbf{R}\mathbf{I}(t) + \mathbf{Z}_p\mathbf{I}(t) + 2\mathbf{V}_p^i[\mathbf{1}]_{N_l} \\ + \mathbf{Z}_m\mathbf{M}(t) + 2\mathbf{V}_m^i[\mathbf{1}]_{3N_m}, \end{aligned} \tag{14}$$

where $\mathbf{Z}_p$ and $\mathbf{Z}_m$ represent the equivalent surge impedances for the inductors $\mathbf{L}_p$ and $\mathbf{L}_m$, respectively. $\mathbf{V}_p^i$ and $\mathbf{V}_m^i$ describe the incident volatges for each inductor element and $[\mathbf{1}]_{N_l}$ and $[\mathbf{1}]_{3N_m}$ represent vectors with elements equal to 1, having sizes N_l and $3N_m$ respectively. The nodal potentials can be represented using capacitive branches, and by applying KVL, the modified form of equation (7) can be expressed as:

$$ \Phi(t) = \mathbf{Z}_c\mathbf{A}^T\mathbf{I}(t) + \mathbf{Z}_c\mathbf{I}_s(t) + 2\mathbf{V}_c^i[\mathbf{1}]_{N_n}. \tag{15}$$

$\mathbf{Z}_c$ represents the equivalent surge impedance for the capacitors in the conventional PEEC circuit, which is the reciprocal of $\mathbf{P}$. $\mathbf{V}_c^i$ is the incident voltage for each capacitor in the TLM model. In the conventional PEEC model, the constitutive relation is expressed as in equation (8), and the system will be solved using the matrix system formulated in equation (10). The non-linear constitutive relation and its corresponding equivalent circuit model, along with the TLM model, are depicted in Fig. 3. In this work, the existing constitutive equation is modeled as an equivalent circuit, as shown in Fig. 3(d), and the non-linearity is represented by the diagonal matrix $\Omega(|H(t)|)$ with size $3Nm$, which can be

This article has been accepted for publication in IEEE Transactions on Magnetics. This is the author's version which has not been fully edited and content may change prior to final publication. Citation information: DOI 10.1109/TMAG.2024.3447621

identified as a non-linear resistor in the network. The non-linear resistor is decoupled from the linear network by using loss-less transmission lines with an arbitrary surge impedance Zu. Fig. 3(f) illustrates the Thevenin equivalent circuit of the non-linear constitutive relation. Consequently, the equivalent representation of equation (11) can be expressed as:

$$\mathbf{D}\mathbf{I}(t) + (\mathbf{W}+\mathbf{Z}_u)\mathbf{M}(t) = -\mathbf{G}\mathbf{I}_s(t) - 2\mathbf{V}_u^i[\mathbf{1}], \tag{16}$$

where $\mathbf{V}_u^i$ is the incident voltage for $3N_m$ nonlinear magnetic elements. Equations (14), (15), and (16) represent the fundamental equations of the proposed TLM-PEEC method, which are used to formulate a matrix system. In the conventional PEEC solver, the final matrix system has the solution vector denoted as $\mathbf{I}(t)$, $\Phi(t)$, and $\mathbf{M}(t)$, as described in [14]. This requires solving for a total of $N_l + N_n + 3N_m$ unknowns. However, in the TLM-PEEC solver, the $\Phi(t)$ vector can be excluded from the KVL equations. Consequently, the solution vector consists solely of $\mathbf{I}(t)$ and $\mathbf{M}(t)$, which corresponds to a total of $N_l + 3N_m$ unknowns. If the solution for $\Phi(t)$ is needed, it can be post-processed using (15) at the desired time step. The final matrix system can be expressed as:

$$\begin{bmatrix} \mathbf{R}+\mathbf{Z}_p+\mathbf{A}\mathbf{Z}_c\mathbf{A}^T & \mathbf{Z}_m \\ \mathbf{D} & \mathbf{W}+\mathbf{Z}_u \end{bmatrix} \begin{bmatrix} \mathbf{I}(t) \\ \mathbf{M}(t) \end{bmatrix} = \begin{bmatrix} -\mathbf{V}_s - 2\mathbf{V}_p^i[\mathbf{1}]_{N_l} - 2\mathbf{V}_m^i[\mathbf{1}]_{3N_m} - 2\mathbf{A}\mathbf{V}_c^i[\mathbf{1}]_{N_n} - 2\mathbf{A}\mathbf{Z}_c\mathbf{I}_s \\ -\mathbf{G}\mathbf{I}_s(t) - 2\mathbf{V}_u^i[\mathbf{1}]_{N_n} \end{bmatrix}. \tag{17}$$

This equation can be solved separately if $\mathbf{V}_u^i$, the incident voltage for magnetic elements, is known for each time step. The unknown incident voltage matrices $\mathbf{V}_p^i$, $\mathbf{V}_m^i$, and $\mathbf{V}_c^i$ can be updated iteratively using linear TLM iterations as described in Section III.A. The linear TLM iteration equation can be written as below.

$$\begin{aligned} {}_n\mathbf{V}_p &= 2{}_n\mathbf{V}_p^i + \mathbf{Z}_p\mathbf{I}_{sq}(t), \\ {}_n\mathbf{V}_p^r &= {}_n\mathbf{V}_p - {}_n\mathbf{V}_p^i, \\ {}_{n+1}\mathbf{V}_p^i &= -{}_n\mathbf{V}_p^r. \end{aligned} \tag{18}$$

$$\begin{aligned} {}_n\mathbf{V}_m &= 2{}_n\mathbf{V}_m^i + \mathbf{Z}_m\mathbf{M}_{sq}(t), \\ {}_n\mathbf{V}_m^r &= {}_n\mathbf{V}_m - {}_n\mathbf{V}_m^i, \\ {}_{n+1}\mathbf{V}_m^i &= -{}_n\mathbf{V}_m^r. \end{aligned} \tag{19}$$

$$\begin{aligned} {}_n\mathbf{V}_c &= 2{}_n\mathbf{V}_c^i + \mathbf{Z}_c\mathbf{I}_{c,sq}(t), \\ {}_n\mathbf{V}_c^r &= {}_n\mathbf{V}_c - {}_n\mathbf{V}_c^i, \\ {}_{n+1}\mathbf{V}_c^i &= {}_n\mathbf{V}_c^r. \end{aligned} \tag{20}$$

$\mathbf{I}_{sq}(t)$, $\mathbf{I}_{c,sq}(t)$ $\mathbf{M}_{sq}(t)$ represent the diagonal matrices formulated from the inductive branch current $\mathbf{I}(t)$, the capacitive branch current $\mathbf{I}_c(t)$ and the magnetization $\mathbf{M}(t)$ respectively. According to TLM theory, nonlinear elements in the circuit can be modeled using (13). The same theory can be applied to Fig. 3d to obtain the nonlinear relationship for the PEEC nonlinear system, which can be written as follows.

$$f({}_{n+1}\mathbf{V}_u^i) = {}_{n+1}\mathbf{V}_u^i + {}_n\mathbf{V}_u^r - \Omega({}_{n+1}\mathbf{V}_u^i)\left(\frac{{}_{n+1}\mathbf{V}_u^i - {}_n\mathbf{V}_u^r}{\mathbf{Z}_u}\right) = 0. \tag{21}$$

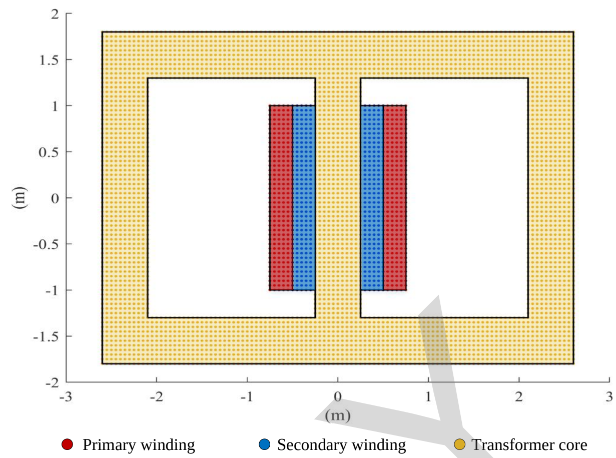

Fig. 4. PEEC node mesh of the 2-D transformer.

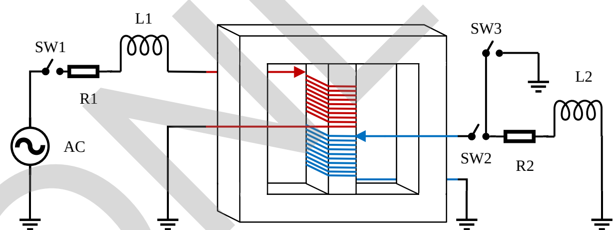

Fig. 5. Schematic of the transformer PEEC model coupled with external networks.

Vector ${}_{n+1}\mathbf{V}_u^i$ with size $3N_m$ represents the incident voltage for the $3N_m$ nonlinear magnetic elements. $\mathbf{V}_u^r$ represents the corresponding reflected voltages, and $\mathbf{Z}_u$ represents the arbitrary surge impedance vector for each nonlinear element. Computing the $\mathbf{V}_u^i$ vector necessitates solving the nonlinear equation using an iterative approach such as the N-R method.

D. N-R Implementation

The solution to the nonlinear TLM equation will be obtained by implementing the N-R algorithm, and by employing proper initial values, the equation can be effectively solved in fewer iterations. Inside the N-R iterations, the value of $\mathbf{I}(t)$ obtained from equation (17), $\mathbf{V}_u^r$ obtained from TLM iterations will be inserted into the subsequent equation to compute the magnetic flux density vector $\mathbf{B}(t)$:

$$\mathbf{B(t)} = \mathbf{DI(t)} + \mathbf{W}\left(\frac{{}_{n+1}\mathbf{V}_u^i - {}_n\mathbf{V}_u^r}{\mathbf{Z}_u}\right), \tag{22}$$

According to the B-H relationship of the magnetic material, the magnetic field vector $\mathbf{H}(t)$ can be obtained and then plugged into equation (8) to calculate $\Omega({}_{n+1}\mathbf{V}_u^i)$. The Jacobian vector for the N-R implementation can be obtained as follows:

$$\frac{\partial f}{\partial_{n+1}\mathbf{V}_u^i} = 1 - \frac{\Omega({}_{n+1}\mathbf{V}_u^i)}{\mathbf{Z}_u} - \frac{\partial \Omega}{\partial_{n+1}\mathbf{V}_u^i}\left(\frac{{}_{n+1}\mathbf{V}_u^i - {}_n\mathbf{V}_u^r}{\mathbf{Z}_u}\right). \tag{23}$$

This equation can be further simplified using the chain rule below;

$$\frac{\partial \Omega}{\partial_{n+1}\mathbf{V}_u^i} = \frac{\partial \Omega}{\partial_{n+1}\mu_r}\frac{\partial_{n+1}\mu_r}{\partial_{n+1}\mathbf{V}_u^i}. \tag{24}$$

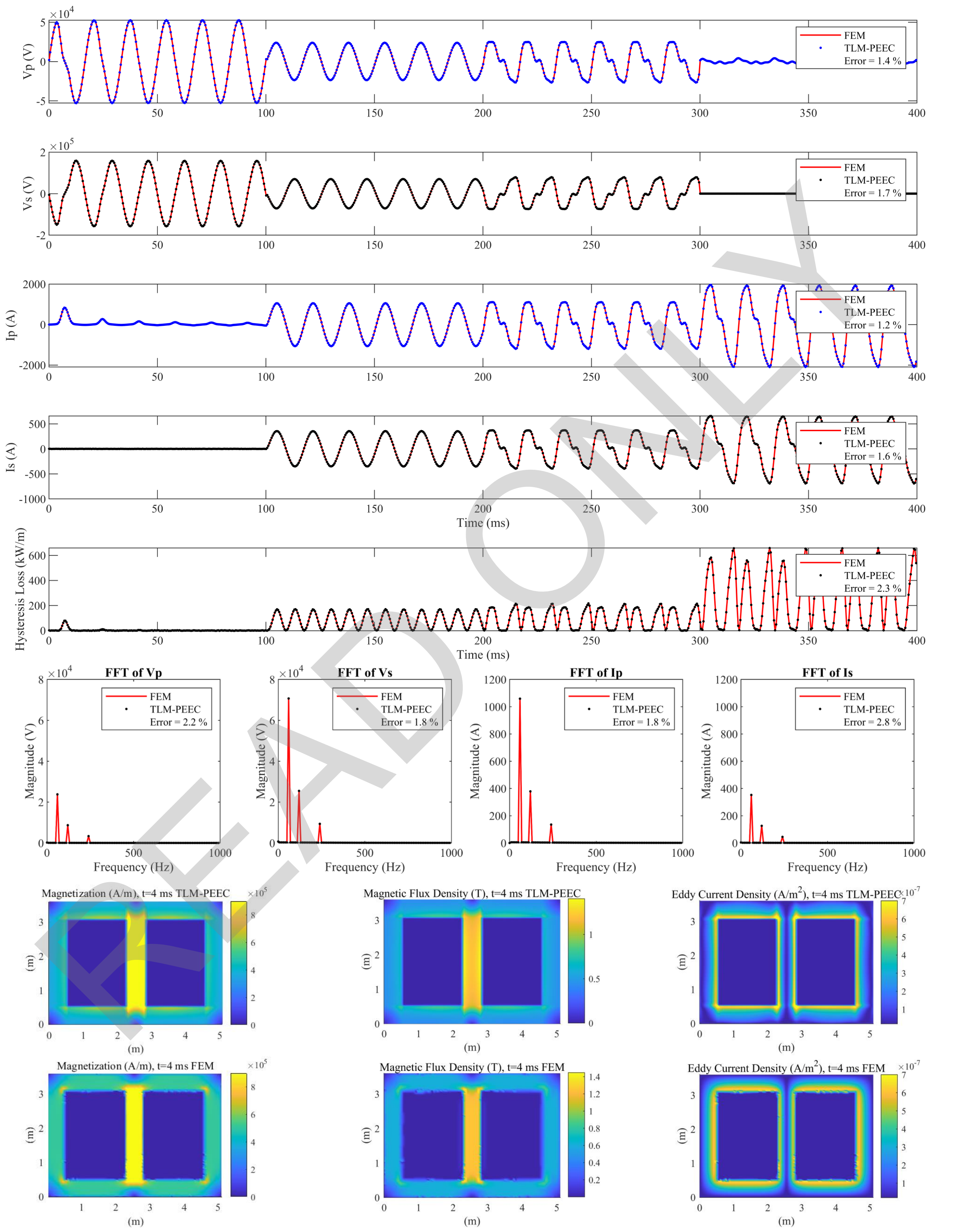

Fig. 6. GPU simulation results of the proposed TLM-PEEC method and the comparison with Comsol results for the Case Study.

After simplifying (24), it can be formulated as follows:

$$\frac{\partial \Omega}{\partial_{n+1}\mathbf{V}_u^i} = \frac{\mu_0}{({}_{n+1}\mu_r - 1)^2}\frac{\mathbf{B} - W \cdot \left(\frac{{}_{n+1}\mathbf{V}_u^i - {}_n\mathbf{V}_u^r}{\mathbf{Z}_u^2}\right)}{\mathbf{B} - \mu_0\left(\frac{{}_{n+1}\mathbf{V}_u^i - {}_n\mathbf{V}_u^r}{\mathbf{Z}_u^2}\right)^2}. \tag{25}$$

Equations (23) and (25) describe the Jacobian for the N-R implementation. With a proper initial guess for the incident voltage vector, it can be solved iteratively to achieve convergence for the incident voltage pulse for the next time step. In the conventional PEEC approach, a full N-R method is used for an $N_l + N_n + 3N_m$-sized matrix system, which is highly computationally intensive during N-R iterations. However, according to our proposed architecture, N-R iterations involve $3N_m$ -sized vectors, and as vector operations proceed, all the nonlinear elements are solved in parallel.

IV. Case study and results

A. Case Study Setup

A single-phase shell-type power transformer was studied in this work with 4749 nodes in the PEEC mesh as illustrated in Fig. 4. The schematic of the TLM-PEEC transformer model coupled to external networks is shown in Fig. 5. External networks are directly connected to both the primary winding PEEC circuit and the secondary winding PEEC circuit, respectively, without involving field circuit coupling methods, as typically seen in FEM. The primary winding is energized by a 60 Hz AC voltage source, and several harmonics are introduced within the simulation model to observe transient behaviors. The relative tolerance of the TLM-PEEC nonlinear solver is set to 10^{-5} to ensure convergence and the applied time step is $100\mu s$. The detailed simulation parameters are available in the appendix. For the Case Study, the total simulation is set to 400 ms and the following events are simulated in between.

1) t = 0 ms, $SW1$ is turned on and the transformer is energized while the secondary winding is open-circuited.
2) t = 100 ms, $SW2$ is turned on and the transformer works with a load of $R2$ and $L2$.
3) t = 200 ms, the second and the fourth harmonics are injected into the voltage source V_{ac}.
4) t = 300 ms, $SW3$ is turned on and the secondary winding is short-circuited.

B. Results and Validation

The case study was implemented using the proposed TLM-PEEC method and executed on the Nvidia Tesla V100 GPU, utilizing the compute unified device architecture (CUDA) with 4749 mesh nodes. To ensure accuracy and speed comparison, a similar benchmark study was conducted using the FEM software Comsol Multiphysics®. FEM is selected for its demonstrated efficiency and reliability as a commercially available benchmark in the power industry, thereby enhancing the applicability of our proposed architecture compared to other numerical methods. FEM is widely utilized in field-oriented electromagnetic transient simulations in power systems [22], making it highly suitable for benchmarking the

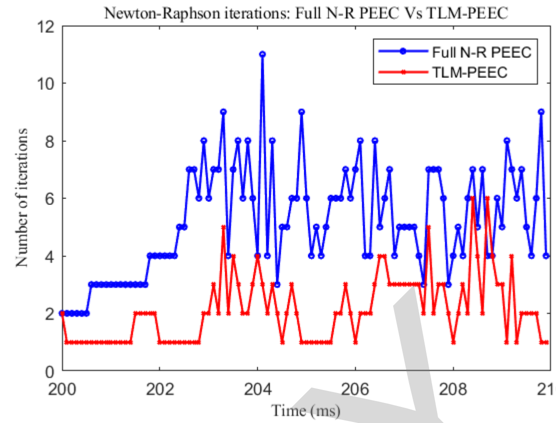

Fig. 7. Comparision of N-R iteration count between full N-R PEEC approach and TLM-PEEC approach.

transformer case study. All partial element calculations and matrix filling operations were performed in parallel by implementing device functions on the GPU. The Nvidia cuSOLVER application programming interface (API) facilitated solving the linear system, while the device functions for matrix addition and multiplication were implemented using first principles. The offline simulation results include primary winding voltage (V_p), secondary winding voltage (V_s), primary winding current (I_p), secondary winding current (I_s), and hysteresis loss. These results are presented in Fig. 6 with a comparison to the corresponding results obtained from Comsol. All errors in the figure denote the mean absolute relative error between the TLM-PEEC solver and the Comsol solver. The results obtained from the Fast Fourier transform (FFT) for the electrical parameters during the harmonic injection period closely match those obtained from Comsol.

The direct outputs from the TLM-PEEC solver consist of transformer winding currents and core magnetization. All other field variables can be derived through PEEC post-processing. Magnetic flux density can be easily obtained from equation (22). The estimation of hysteresis losses in the core can be conducted by following the approach presented in [23]. The determination of the electric field using the PEEC method is not straightforward, and the extraction of the electric field within the core followed the approach detailed in [24]. Subsequently, this electric field information can be utilized in the following equation to calculate the eddy current density:

$$L_{eddy} = \int\int_{\Omega_{core}} \sigma^2 E^2 d\Omega_{core}. \tag{26}$$

The eddy current density was computed by estimating the integral as a summation over the surface area of the core. The detailed field distributions of magnetization M (A/m), magnetic flux density B (T), and eddy current density J (A/m²) at t = 4 ms were obtained from both the TLM-PEEC solver and Comsol simulations, and their comparison is illustrated in Fig. 6. The comparison of the occupied maximum N-R iteration count for the full N-R PEEC approach and the TLM-PEEC approach at each time step is illustrated in Fig. 7 for the 200 ms - 210 ms time window within the

TABLE I
TLM-PEEC EXECUTION TIME AND SPEEDUP ON MANY-CORE GPU AND MULTI-CORE CPU

Cases	Number of Nodes	Comsol™ Execution Time (s)	TLM-PEEC on many-core GPU		TLM-PEEC on multi-core CPU	
			Execution Time (s)	Speedup	Execution Time (s)	Speedup
Case 1	3610	93.1	2.1	44.3	9.0	10.3
Case 2	4749	120.2	3.1	38.7	12.2	9.9
Case 3	6816	219.0	6.9	31.7	23.0	9.5
Case 4	11461	418.4	24.2	17.3	47.5	8.8
Case 5	24174	1627.2	102.7	15.8	200.8	8.1
Case 6	92579	6603.6	475.4	13.9	880.5	7.5

harmonic injection period. The results show that the TLM-PEEC approach required fewer N-R iterations for convergence. Furthermore, the TLM-PEEC method utilizes a decoupled N-R approach that solves the nonlinear circuit using $2N_m$-sized vectors, resulting in performance improvements.

The Comsol simulation was carried out on a PC equipped with an Intel Xeon E5-2698 CPU with 40 cores, operating at a clock frequency of 2.2 GHz, and equipped with 192 GB of RAM, as it cannot be executed on a GPU [25]. The Comsol solver is designed to utilize the maximum available cores in the multi-core CPU [26], providing a parallel CPU benchmark simulation for performance comparison of the TLM-PEEC on the GPU. A pthread implementation of the proposed TLM-PEEC method was conducted on the same multi-core CPU platform to evaluate its performance on identical hardware. The pthread library was chosen for its efficient creation and management of parallel threads. To ensure consistency with the case study environment, the tolerance of the Comsol solver was set to 10^{-5}. The total simulation duration was 400 ms, with a time step of 100 us. For this specific case study, the Comsol simulation took 120.2 seconds, while the TLM-PEEC GPU solver completed the simulation in only 3.1 seconds, and the TLM-PEEC CPU solver completed it in 12.2 seconds, resulting in performance improvements in both GPU and CPU results. Simulations were performed with varying mesh sizes, as outlined in Table I, to further investigate the performance. N-R iteration requires $2N_m$ parallel cores for the given 2D case study to achieve maximum parallelism. The GPU consists of 5120 cores and experiences a substantial speedup decrease after Case 3 due to reaching the maximum core limit. However, the GPU speedup is always greater than the CPU speedup, as the GPU has a large number of cores designed for parallel processing with specialized parallel programming model CUDA, along with higher memory bandwidth.

V. CONCLUSION

In this article, a novel TLM-based parallel time domain solver was successfully integrated into the standard PEEC method. The TLM-based matrix solver was introduced, reducing the unknowns from $N_l + N_n + 3N_m$ to $N_l + 3N_m$ compared to the standard PEEC matrix solver. An efficient computational approach for nonlinear magnetic material modeling introduced a decoupled N-R method, replacing the direct N-R solver. This method is scalable for any application involving magnetic materials, and for 3D nonlinear magnetic materials, it requires $3N_m$ independent calculations for the N-R solver. The numerical results validate the correctness of the proposed approach, demonstrating reliable accuracy with a mean absolute relative error of less than 2% over the entire period achieving a maximum of 44.3x speedup on GPU compared to Comsol. Even though the Comsol solver and the proposed TLM-PEEC solver ran on the same multi-core CPU, the proposed TLM-PEEC solver achieved a maximum speedup of 9.9x compared to Comsol due to the TLM-based decoupled N-R approach being more efficient than the direct N-R approach used inside the Comsol solver. The maximum performance is achieved by solving the nonlinear elements separately, without interacting with the linear elements, resulting in a simpler nonlinear system and easier convergence. The proposed TLM-PEEC approach is applicable to any PEEC problems that can be solved using conventional MNA solvers and is highly beneficial for nonlinear electromagnetic problems as it solves the nonlinear system separately while solving the whole system in parallel. Although the presented case study focused on the 2D modeling of transformers the proposed approach remains applicable and extendable to 3D modeling of electromagnetic apparatus.

APPENDIX A

Transformer parameters: The yoke length is 5.1 m, the limb length is 2.6 m, and the coil size is 0.25m × 2 m. The primary winding consists of 600 turns, while the secondary winding has 200 turns.

Case study parameters: V_{AC} = 53.033sin(60πt) kV, R1 = 25 Ω, R2 = 200 Ω, and L1 = L2 = 36 mH. The magnitude of the injected second and fourth harmonics are 21.76 kV and 10.88 kV at frequencies of 120 Hz and 240 Hz, respectively.

REFERENCES

[1] A. Kalimov, S. Vaznov, and T. Voronina, "Eddy current calculation using finite element method with boundary conditions of integral type," *IEEE Trans. Magn.*, vol. 33, no. 2, pp. 1326–1329, Mar. 1997.

[2] Y. Takahashi and S. Wakao, "Large-scale analysis of eddy-current problems by the hybrid finite element-boundary element method combined with the fast multipole method," *IEEE Trans. Magn.*, vol. 42, no. 4, pp. 671–674, Apr. 2006.

[3] P. Liu, J. Li, and V. Dinavahi, "Matrix-free nonlinear finite-element solver using transmission-line modeling on gpu," *IEEE Trans. Magn.*, vol. 55, no. 7, pp. 1–5, Jul. 2019.

[4] J. Li, P. Liu, and V. Dinavahi, “Massively parallel computation for 3-D nonlinear finite edge element problem with transmission line decoupling technique,” *IEEE Trans. Magn.*, vol. 55, no. 10, pp. 1–8, Oct. 2019.
[5] P. Bettini, M. Passarotto, and R. Specogna, “Coupling volume and surface integral formulations for eddy-current problems on general meshes,” *IEEE Trans. Magn.*, vol. 54, no. 3, pp. 1–4, Mar. 2018.
[6] V. Le-Van, G. Meunier, O. Chadebec, and J.-M. Guichon, “A magnetic vector potential volume integral formulation for nonlinear magnetostatic problem,” *IEEE Trans. Magn.*, vol. 52, no. 3, Mar. 2016, Art. no. 7002804.
[7] A. E. Ruehli, “Inductance calculations in a complex integrated circuit environment,” *IBM J. Res. Develop.*, vol. 16, no. 5, pp. 470–481, Sep. 1972.
[8] A. Ruehli and P. Brennan, “Efficient capacitance calculations for three-dimensional multiconductor systems,” *IEEE Trans. Microw. Theory Techn.*, vol. 21, no. 2, pp. 76–82, Feb. 1973.
[9] A. E. Ruehli, “Equivalent circuit models for three-dimensional multi-conductor systems,” *IEEE Trans. Microw. Theory Techn.*, vol. 22, no. 3, pp. 216–221, Mar. 1974.
[10] A. Ruehli and H. Heeb, “Circuit models for three-dimensional geometries including dielectrics,” *IEEE Trans. Microw. Theory Techn.*, vol. 40, no. 7, pp. 1507–1516, Jul. 1992.
[11] C. Wollenberg and A. Gurisch, “Analysis of 3-d interconnect structures with peec using spice,” *IEEE Trans. Electromagn. Compat.*, vol. 41, no. 4, pp. 412–417, Nov. 1999.
[12] G. Antonini, M. Sabatini, and G. Miscione, “PEEC modeling of linear magnetic materials,” in *Proc. IEEE EMC*, Portland, OR, USA, Aug. 2006, pp. 93–98.
[13] D. Romano and G. Antonini, “Quasi-static partial element equivalent circuit models of linear magnetic materials,” *IEEE Trans. Magn.*, vol. 51, no. 7, pp. 1–15, Jul. 2015.
[14] D. Romano, G. Antonini, and A. E. Ruehli, “Time-domain partial element equivalent circuit solver including non-linear magnetic materials,” *IEEE Trans. Magn.*, vol. 52, no. 9, pp. 1–11, Sep. 2016.
[15] C.-W. Ho, A. Ruehli, and P. Brennan, “The modified nodal approach to network analysis,” *IEEE Trans. Circuits Syst.*, vol. 22, no. 6, pp. 504–509, Jun. 1975.
[16] D. Gope, A. Ruehli, and V. Jandhyala, “Solving low-frequency EM-CKT problems using the PEEC method,” *IEEE Trans. Adv. Packag.,*, vol. 30, no. 2, pp. 313–320, May 2007.
[17] S. Safavi and J. Ekman, “A hybrid PEEC-SPICE method for time-domain simulation of mixed nonlinear circuits and electromagnetic problems,” *IEEE Trans. Electromagn. Compat.*, vol. 56, no. 4, pp. 912–922, Aug. 2014.
[18] P. B. Johns and R. L. Beurle, “Numerical solution of 2-dimensional scattering problems using a transmission-line matrix,” *Proc. Inst. Elect. Eng.*, vol. 118, no. 9, pp. 1203–1208, Sep. 1971.
[19] P. B. Johns and M. O’Brien, “Use of the transmission-line modelling (t.l.m.) method to solve non-linear lumped networks,” *Radio Electron. Eng.*, vol. 50, no. 1.2, pp. 59–70, Jan. 1980.
[20] S. Y. R. Hui and C. Christopoulos, “Numerical simulation of power circuits using transmission-line modelling,” *Proc. Inst. Elect. Eng., Phys. Sci., Meas. Instrum., Manage. Educ.*, vol. 137, no. 6, pp. 379–384, Nov. 1990.
[21] V. Dinavahi, “Transient analysis of systems with multiple nonlinear elements using tlm,” *IEEE Trans. Power Syst.*, vol. 19, no. 4, pp. 2102–2103, Nov. 2004.
[22] S. Liu, Y. Liu, H. Li, and F. Lin, “Diagnosis of transformer winding faults based on FEM simulation and on-site experiments,” *IEEE Trans. Dielectrics Elect. Insul.*, vol. 23, no. 6, pp. 3752–3760, Dec. 2016.
[23] P. Liu and V. Dinavahi, “Real-time finite-element simulation of electromagnetic transients of transformer on FPGA,” *IEEE Trans. Power Del.*, vol. 33, no. 4, pp. 1991–2001, Aug. 2018.
[24] D. Romano, G. Antonini, L. Lombardi, U. Grossner, and I. Kovačević-Badstübner, “Analytical formulas for the computation of the electric field in the partial element equivalent circuit method with conductive, dielectric, and magnetic media,” *IEEE Trans. Magn.*, vol. 55, no. 10, pp. 1–13, Oct. 2019.
[25] “Comsol knowledge base article - 866.” [Online]. Available: https://www.comsol.com/support/knowledgebase/866 (accessed Mar. 1, 2024).
[26] “Comsol documentation - version 6.2.” [Online]. Available: https://doc.comsol.com/6.2/docserver (accessed Mar. 1, 2024).